Electronic Supplementary Material (ESI) for Organic & Biomolecular Chemistry.
This journal is © The Royal Society of Chemistry 2024

Supporting Information

Amino Acids as Bio-Organocatalysts in Ring-Opening Copolymerization for Eco-Friendly Synthesis of Biobased Oligomers from Vegetable Oils

Francisca Werlinger,[a,b] Monserrat Beroíza-Duhart,[b] Oscar A. Douglas-Gallardo,[b] Silvia Oyarzo-Aro,[b] Maria Luisa Valenzuela,[c] Oleksandra S. Trofymchuk,[a]* Mario E. Flores,[b]* and Javier Martínez,[b]*

[a]Facultad de Ciencias Químicas y Farmacéuticas, Departamento de Química Orgánica y Fisicoquímica, Universidad de Chile, Santiago 8380492, Chile.
[b]Instituto de Ciencias Químicas, Facultad de Ciencias, Isla Teja, Universidad Austral de Chile, Valdivia 5090000, Chile.
[c]Universidad Autónoma de Chile, Facultad de Ingeniería, Instituto de Ciencias Químicas Aplicadas, Grupo de Investigación en Energía y Procesos Sustentables, Av. El Llano Subercaseaux, Santiago, 2801, Chile

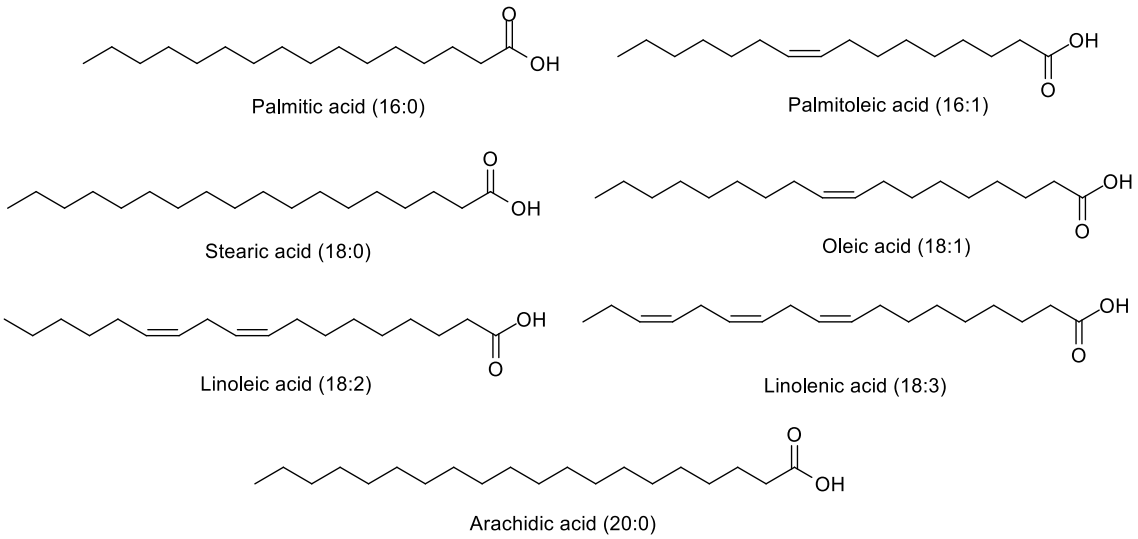

Figure S1. Chemical structures of fatty acids found in waste cooking olive oil, WCOO.

Table S1. Fatty acid composition of cooking olive oil.[a]

(16:0) (%)	(16:1) (%)	(18:0) (%)	(18:1) (%)	(18:2) (%)	(18:3) (%)	(20:0) (%)	Ox. Num. (mmol/g)[a]
12.53	1.02	2.17	72.07	11.10	0.71	0.40	2.92

[a]Determined by GC-FID. [b]Ox. Number: Number of double bonds per gram of triglyceride unit. Ox. Number = (Σ %fatty acid·x)/100; x = total number of double bonds per triglyceride unit.

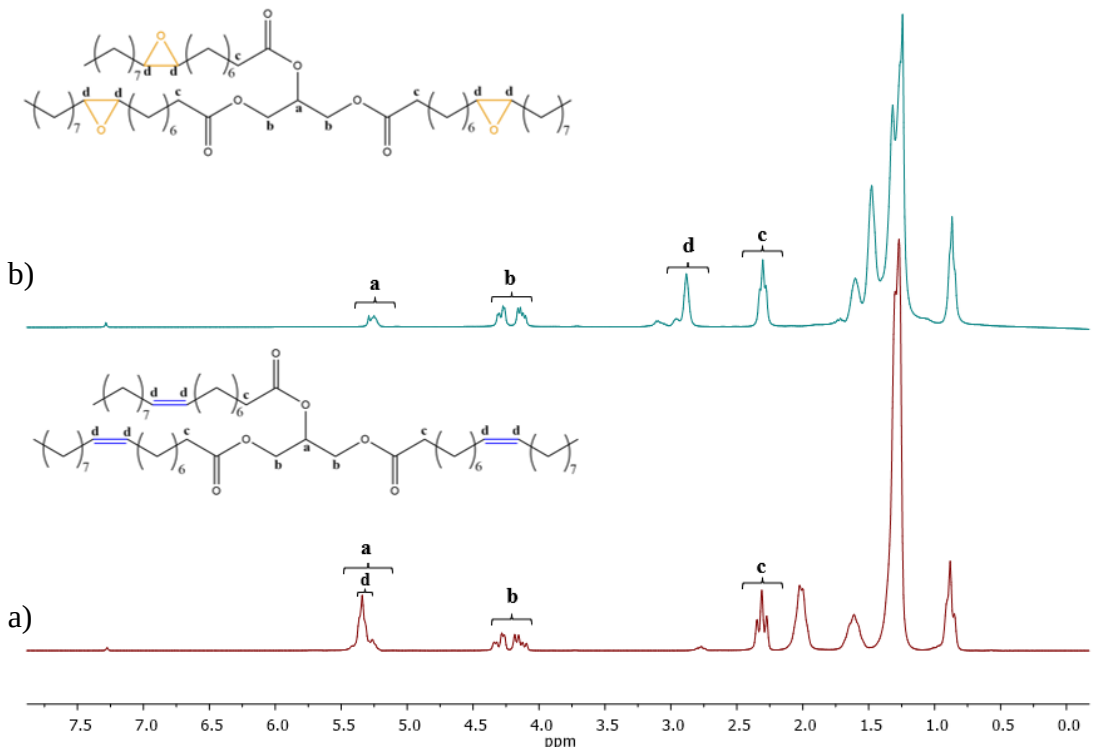

Figure S2. ^{1}H-NMR spectrum of a) waste cooking olive oil, WCOO; b) Epoxidized Olive Oil, EOO in $CDCl_3$.

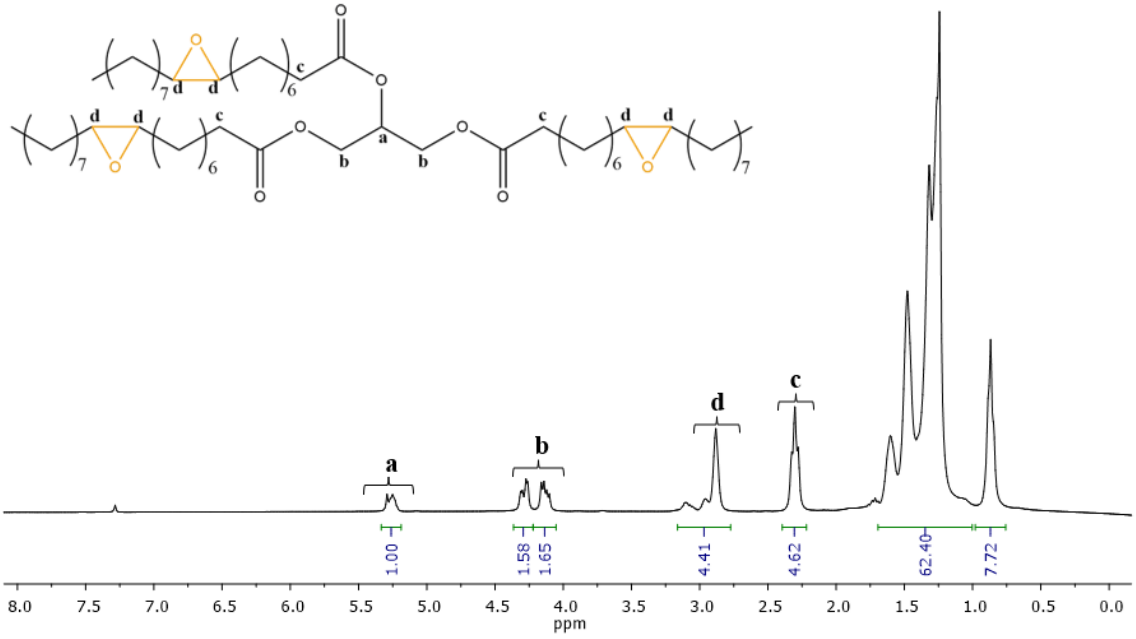

Figure S3. ^{1}H-NMR spectrum of EOO in $CDCl_3$.

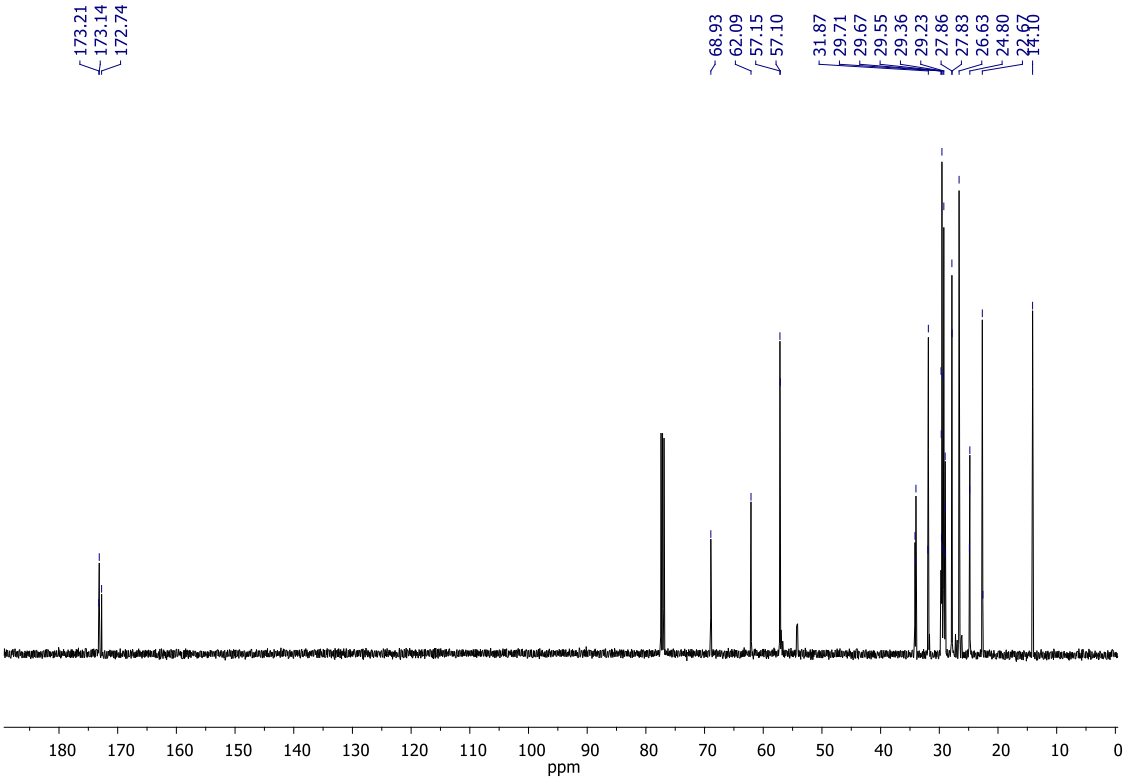

Figure S4. $^{13}C\{^{1}H\}$-NMR spectrum of EOO in $CDCl_3$.

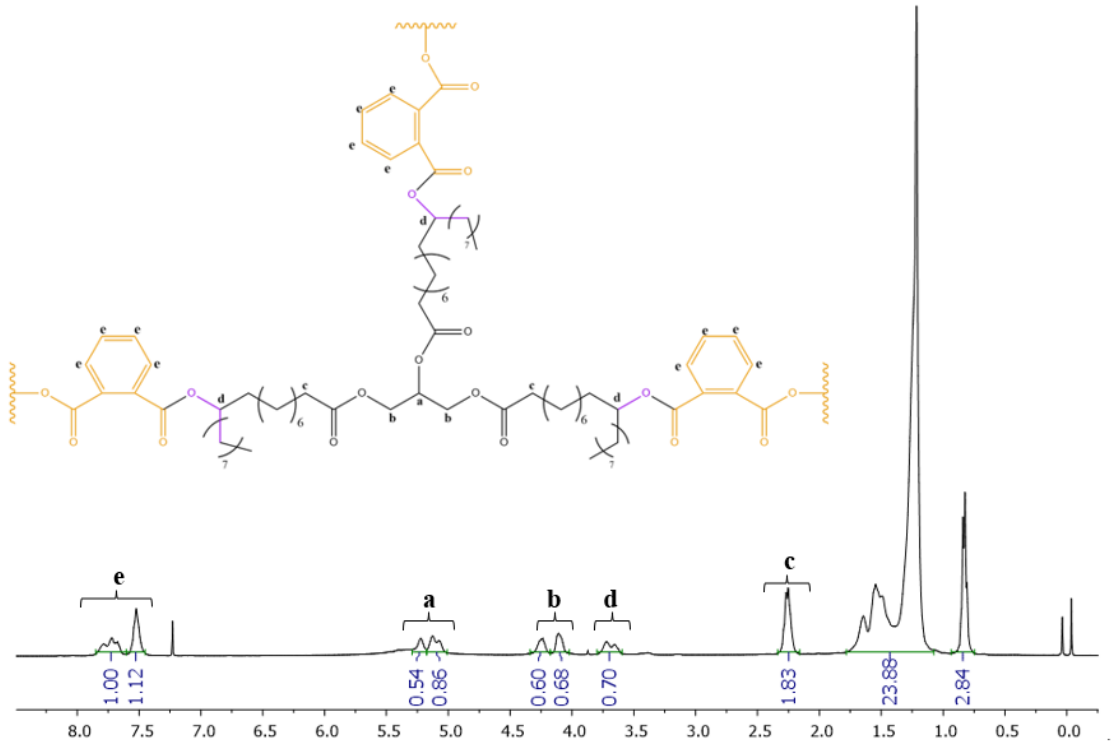

Figure S5. ^{1}H-NMR spectrum of poly(EOO-*co*-PA) in $CDCl_3$.

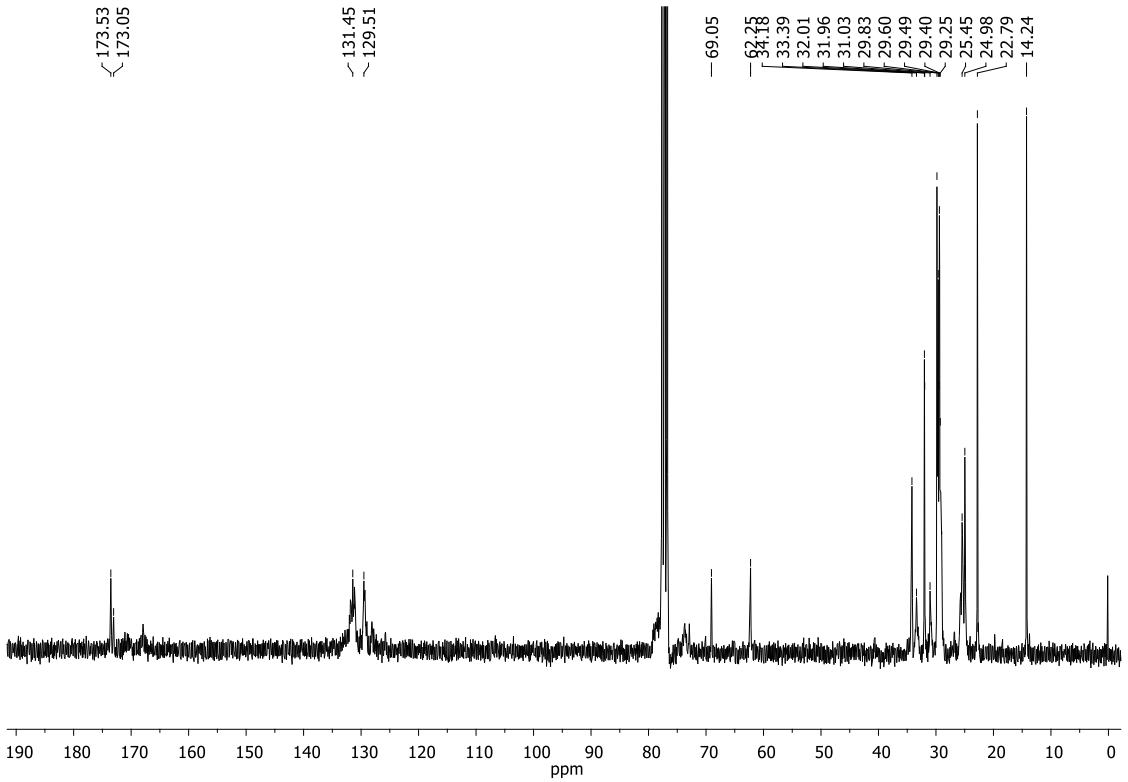

Figure S6. $^{13}C\{^{1}H\}$-NMR spectrum of poly(EOO-*co*-PA) in $CDCl_3$.

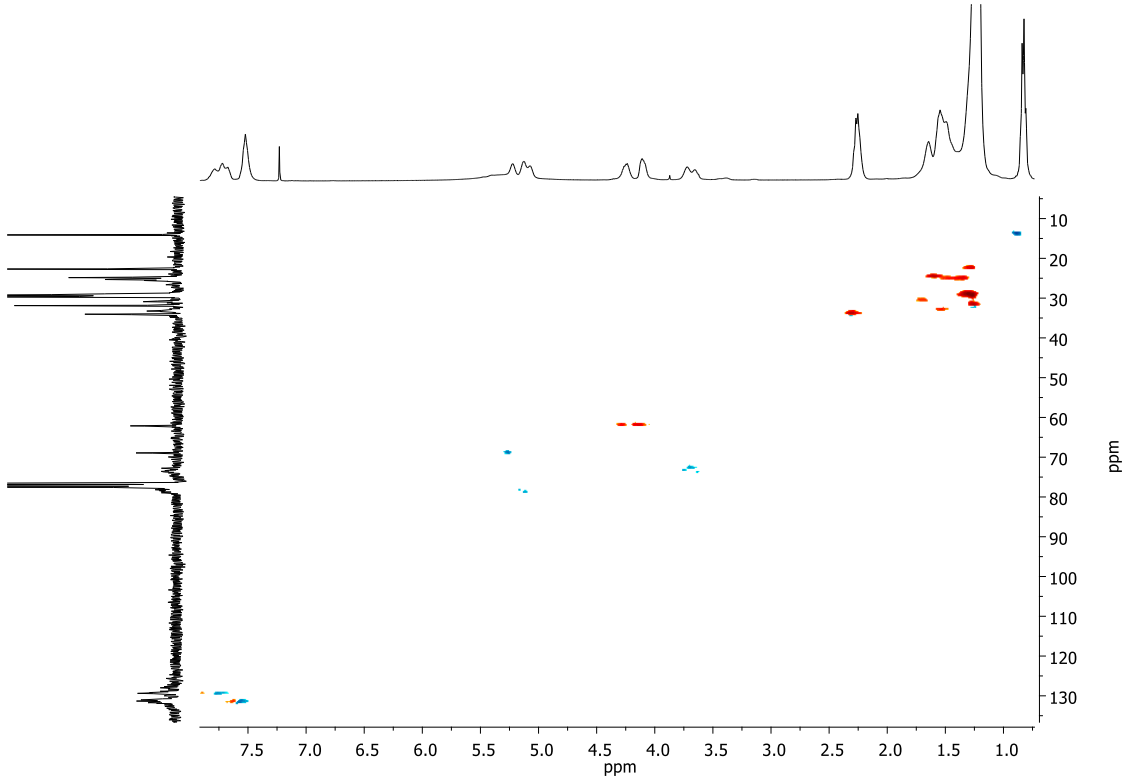

Figure S7. g-HSQC NMR spectrum of poly(EOO-*co*-PA) in $CDCl_3$.

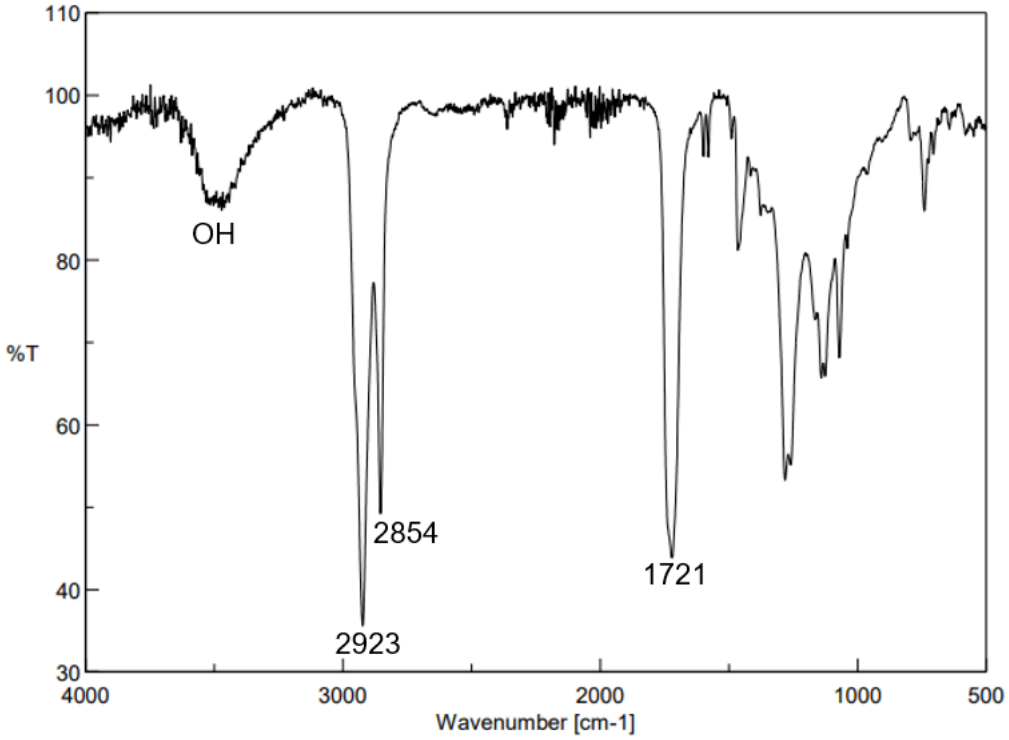

Figure S8. FT-IR spectrum of poly(EOO-*co*-PA) in $CDCl_3$.

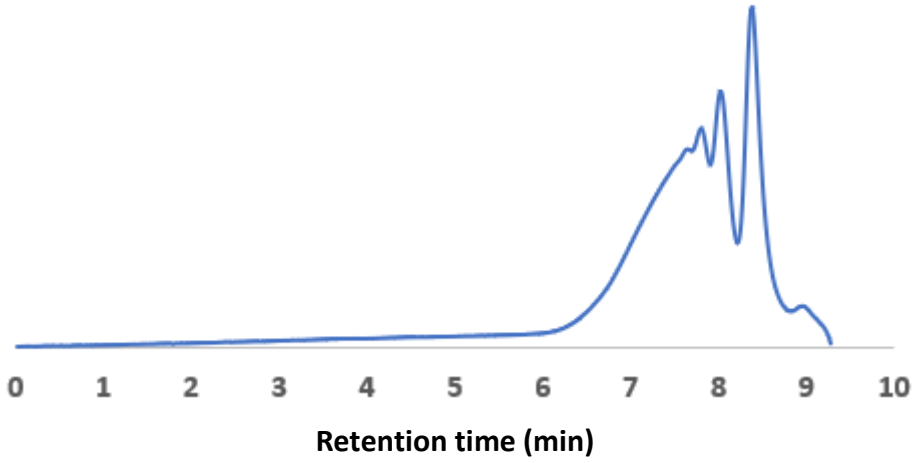

Figure S9. GPC trace of poly(EOO-*co*-PA).

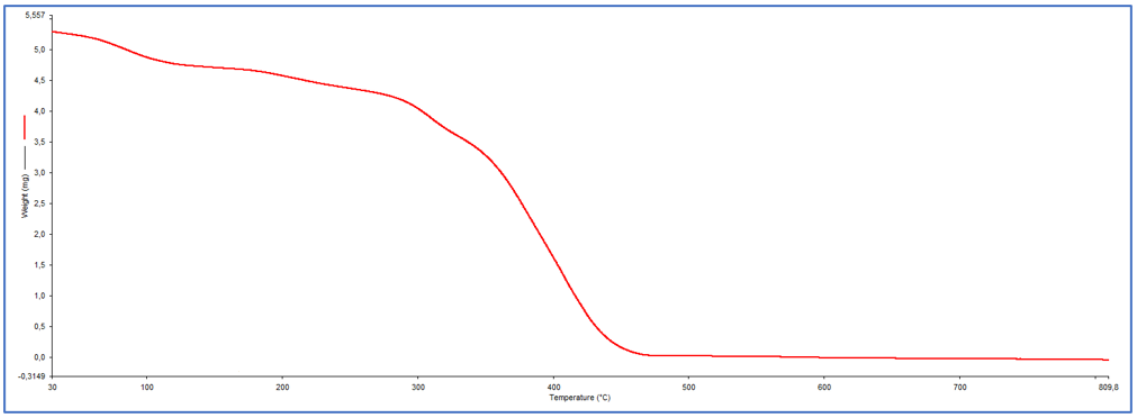

Figure S10. TGA analysis of poly(EOO-*co*-PA).

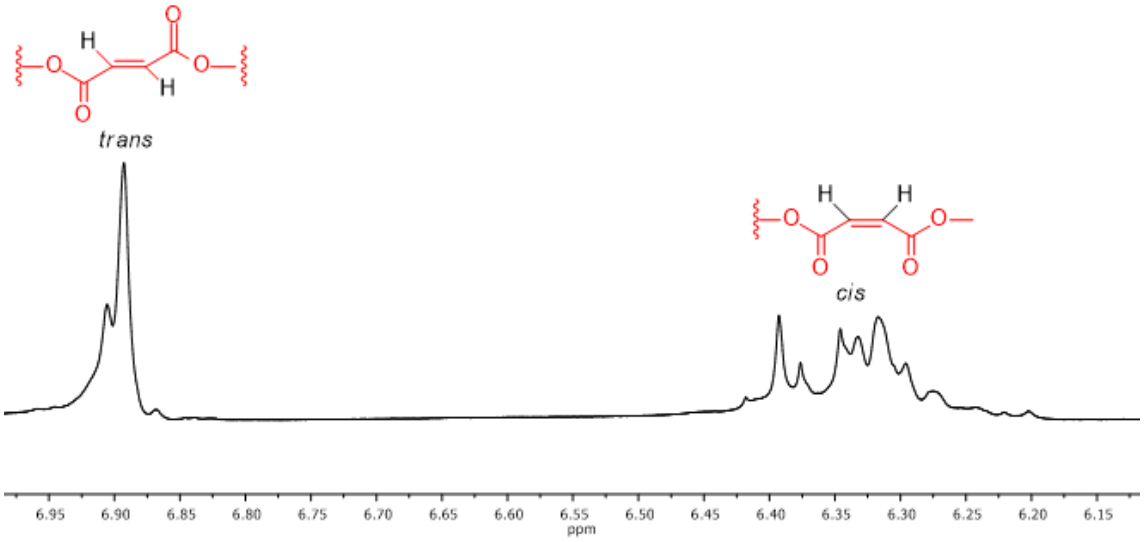

Figure S11. ^{1}H-NMR spectrum of mixture *cis*/*trans* poly(EOO-*co*-MA); Table 2, entry 1

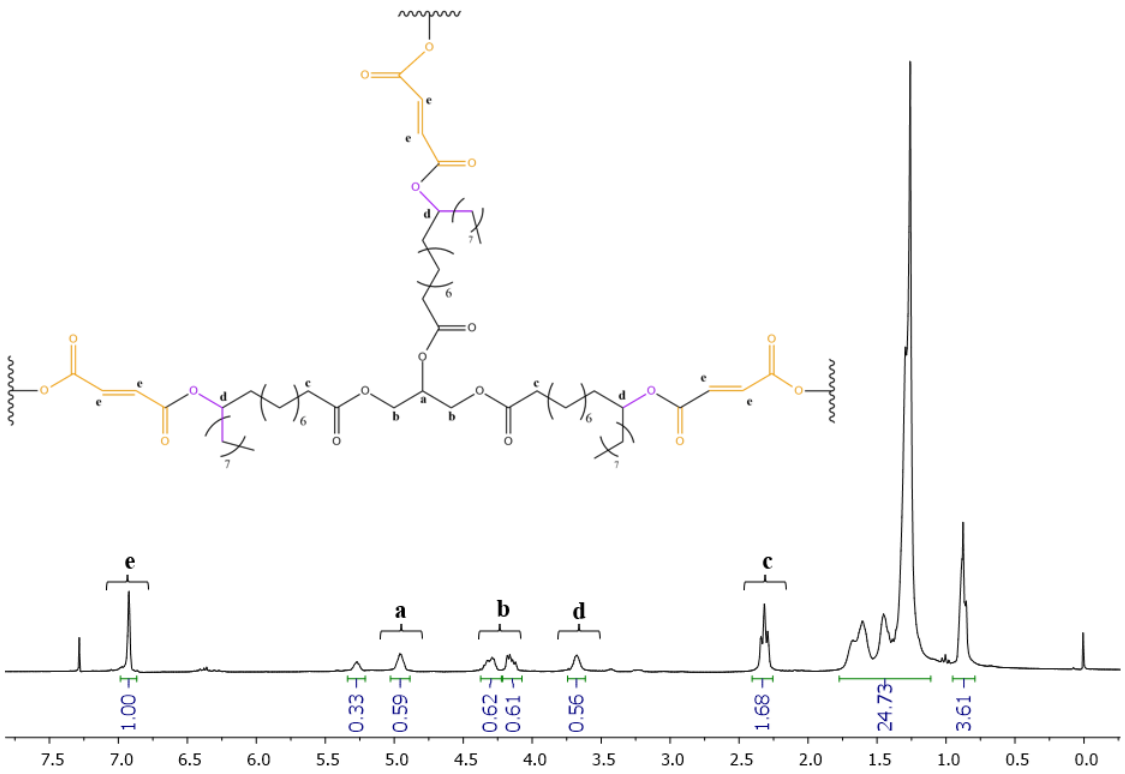

Figure S12. ^{1}H-NMR spectrum of *trans* poly(EOO-*co*-MA) in $CDCl_3$.

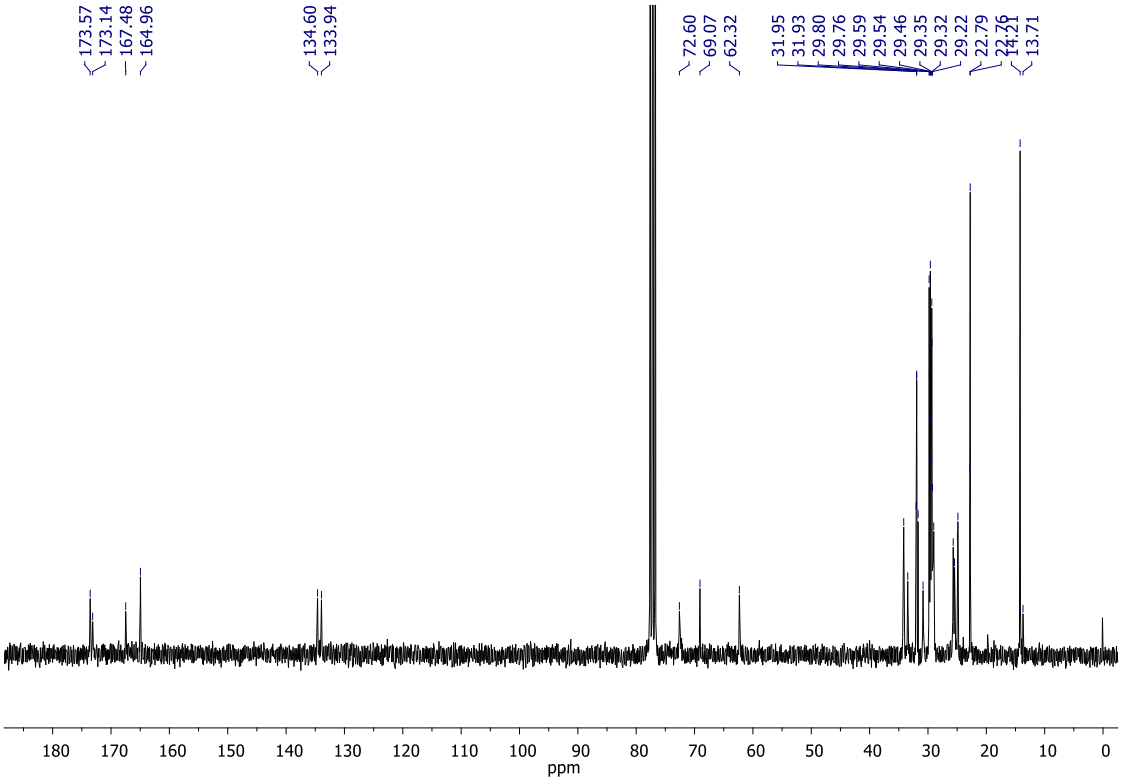

Figure S13. ^{13}C{^{1}H}-NMR spectrum of *trans* poly(EOO-*co*-MA) in $CDCl_3$.

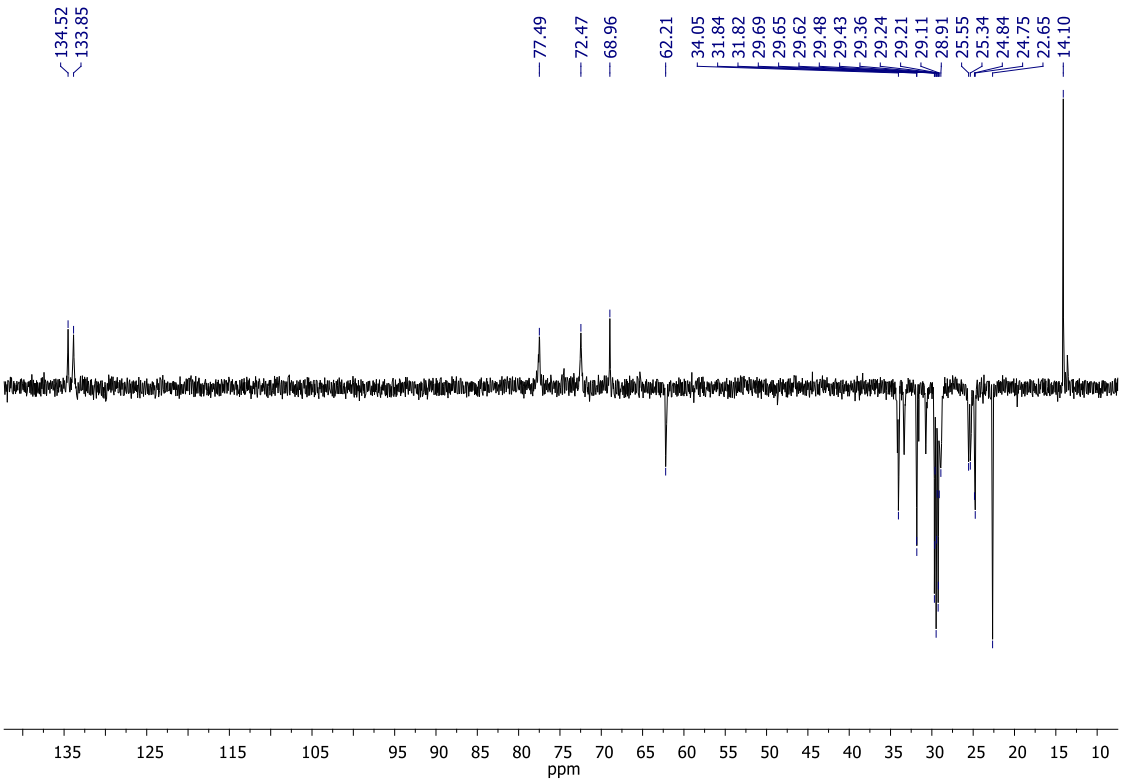

Figure S14. DEPT-NMR spectrum of *trans* poly(EOO-*co*-MA) in $CDCl_3$.

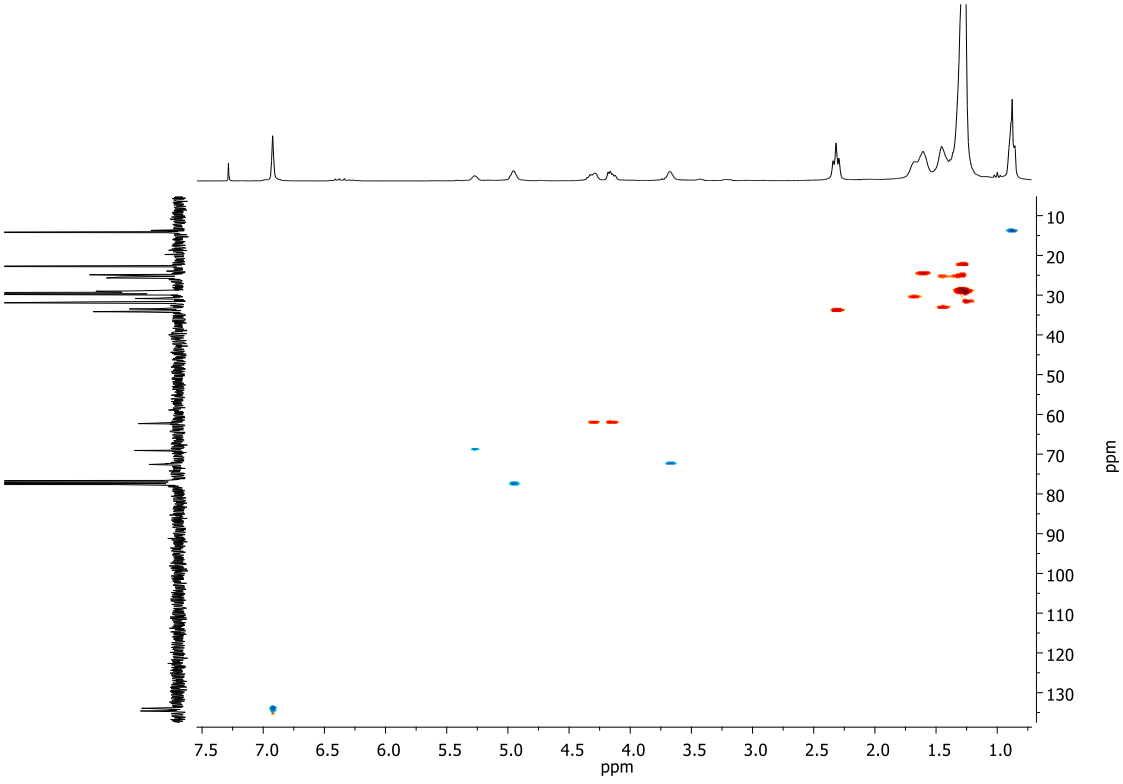

Figure S15. g-HSQC NMR spectrum of poly(EOO-*co*-SA) in $CDCl_3$.

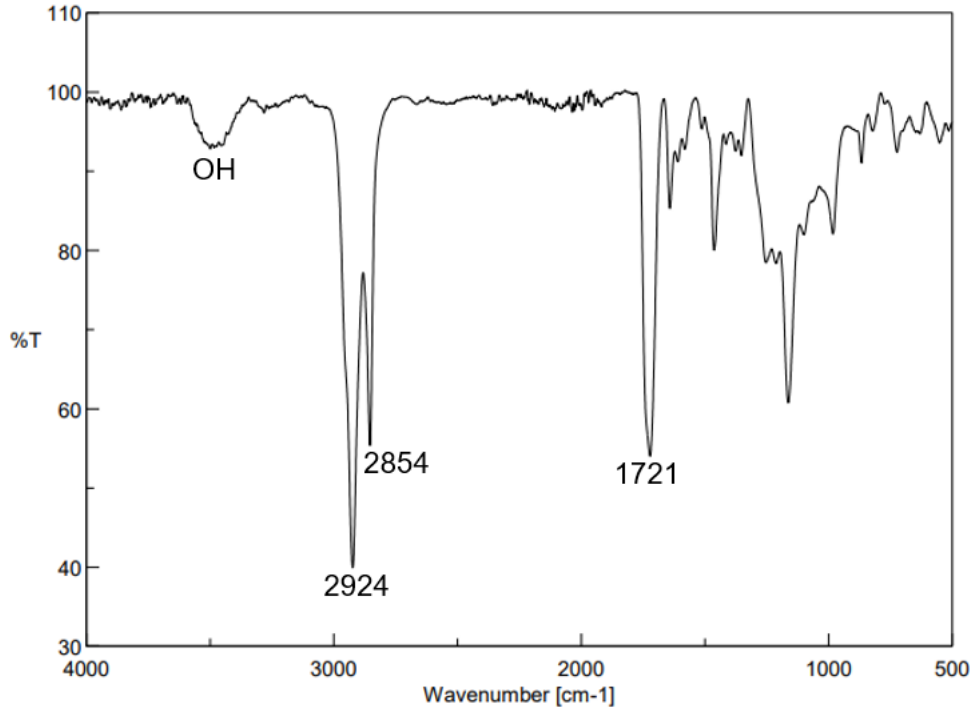

Figure S16. FT-IR spectrum of *trans* poly(EOO-*co*-MA) in $CDCl_3$.

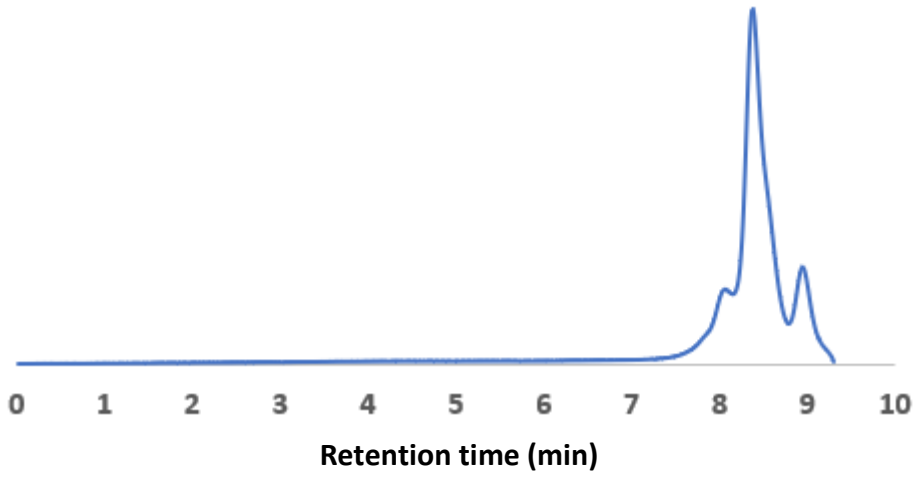

Figure S17. GPC trace of *trans* poly(EOO-*co*-MA).

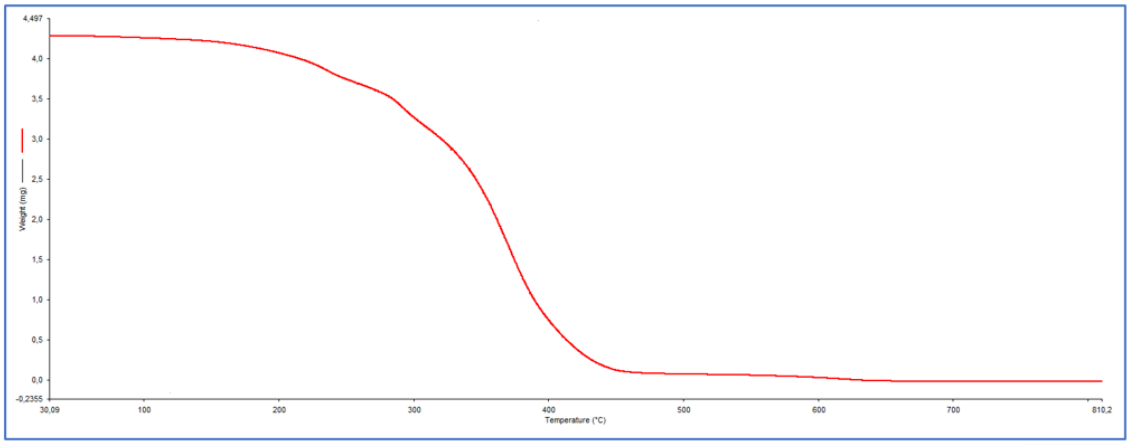

Figure S18. TGA analysis of *trans* poly(EOO-*co*-MA).

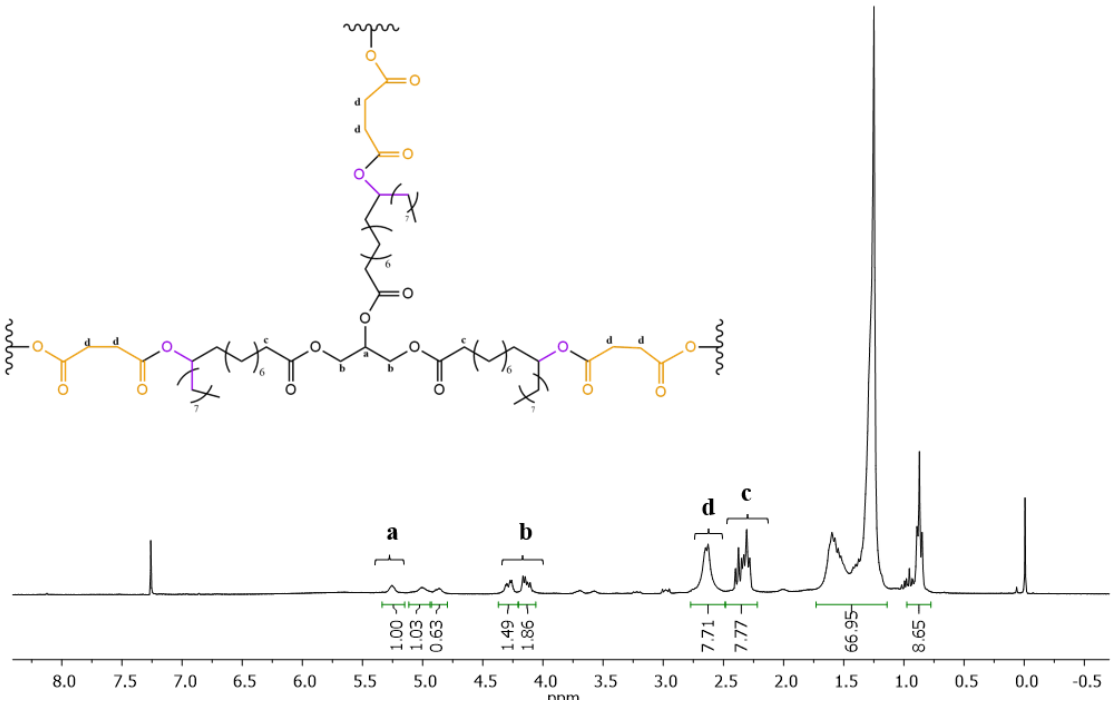

Figure S19. ^{1}H-NMR spectrum of poly(EOO-*co*-SA) in $CDCl_3$.

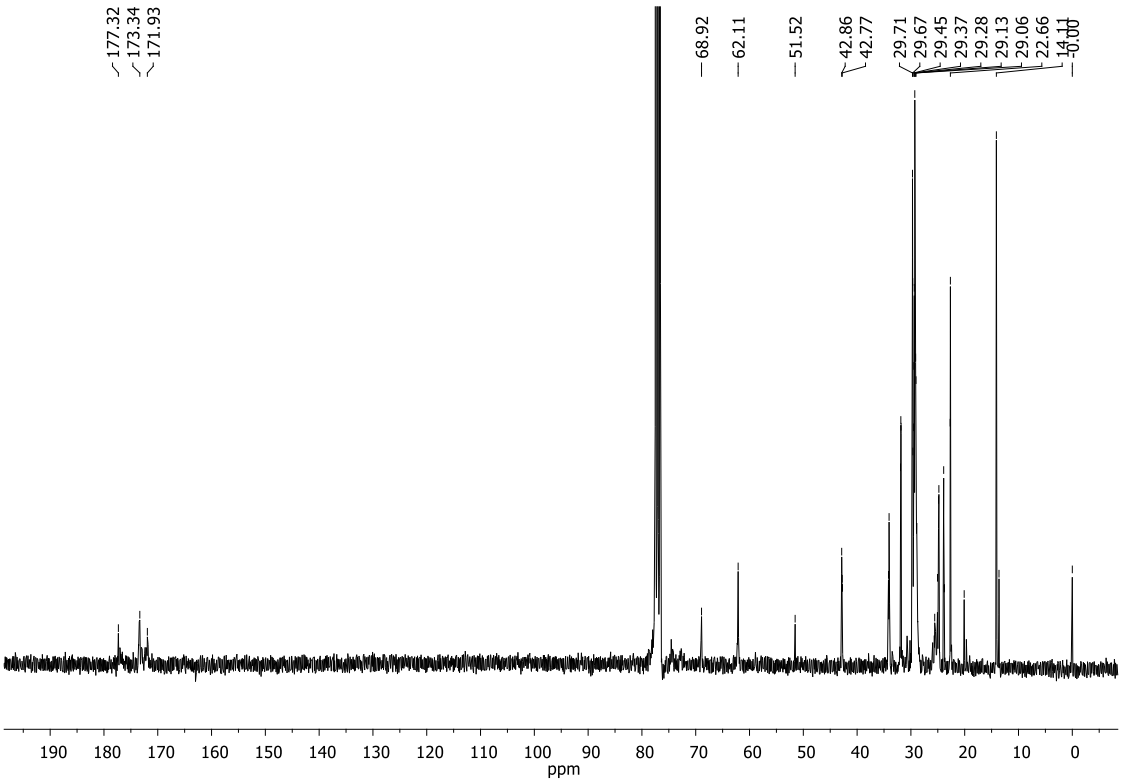

Figure S20. $^{13}C\{^{1}H\}$-NMR spectrum of poly(EOO-*co*-SA) in $CDCl_3$.

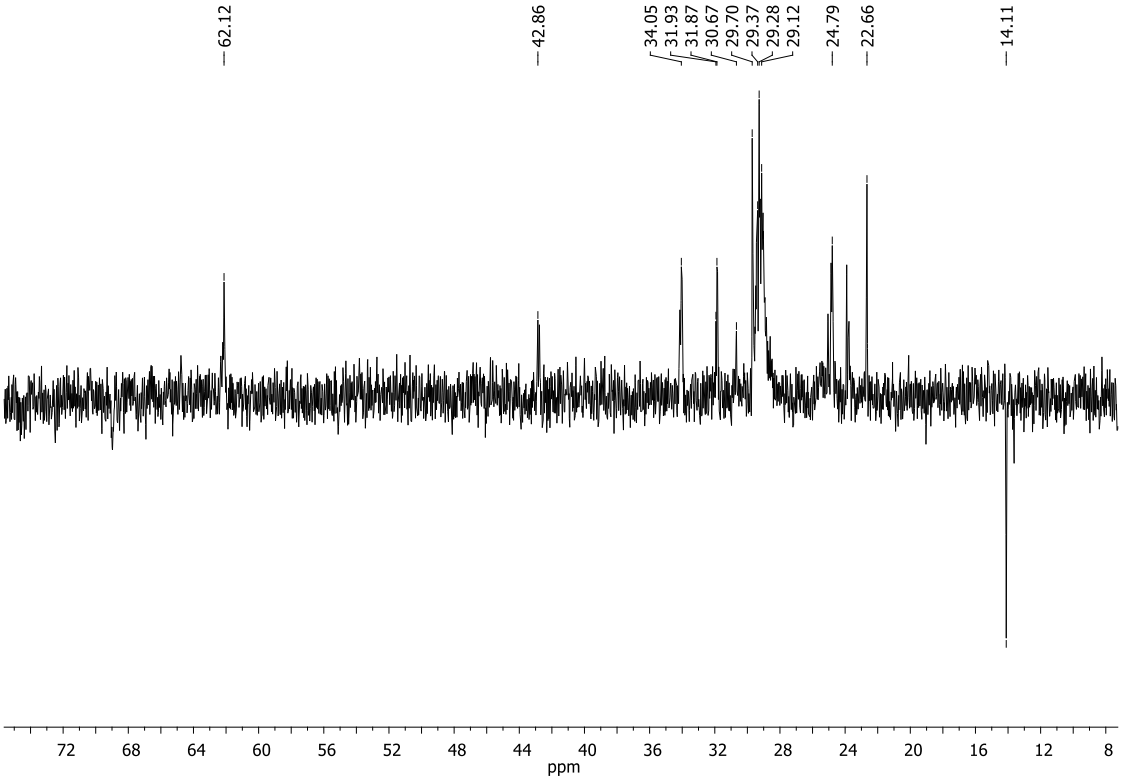

Figure S21. DEPT-NMR spectrum of poly(EOO-*co*-SA) in $CDCl_3$.

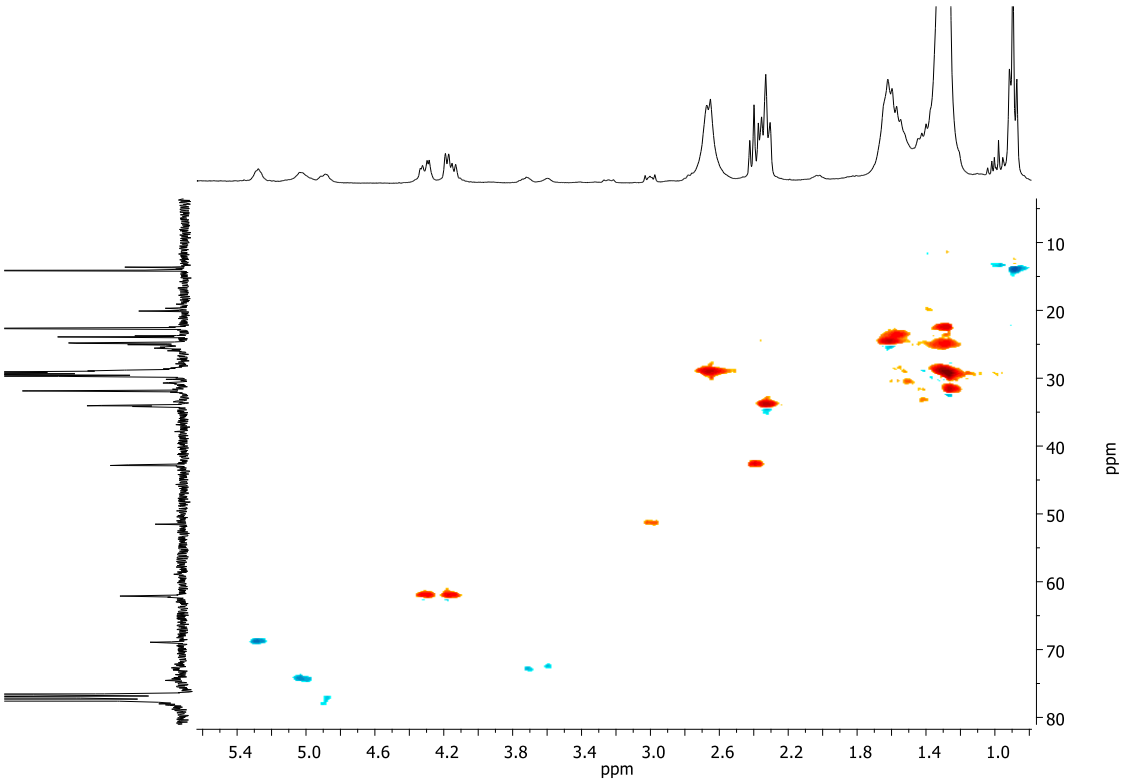

Figure S22. g-HSQC NMR spectrum of poly(EOO-*co*-SA) in $CDCl_3$.

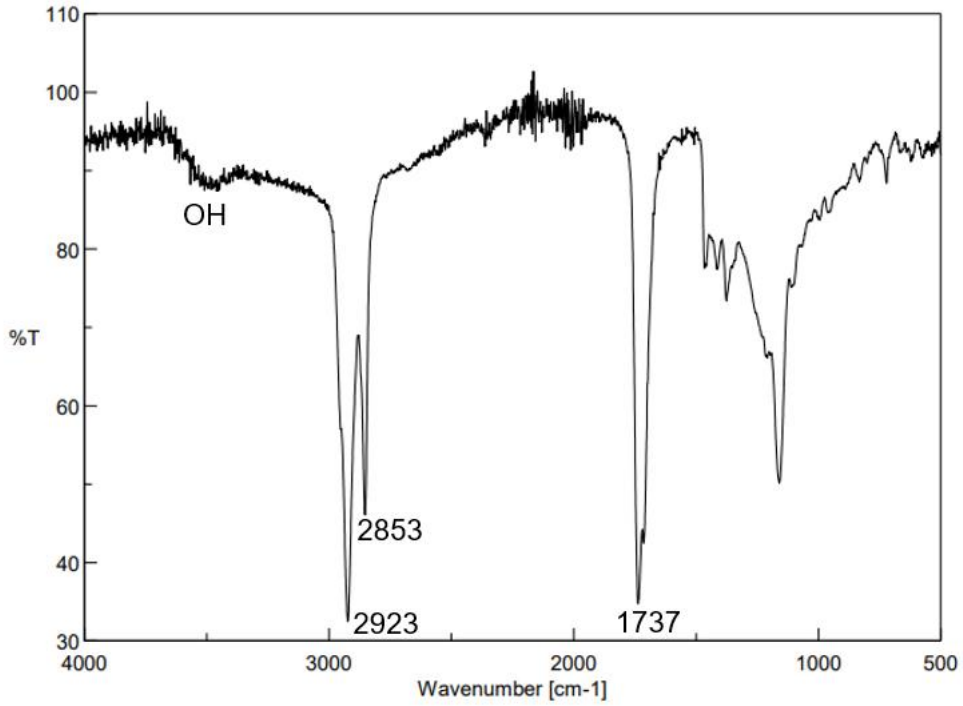

Figure S23. FT-IR spectrum of poly(EOO-*co*-SA) in $CDCl_3$.

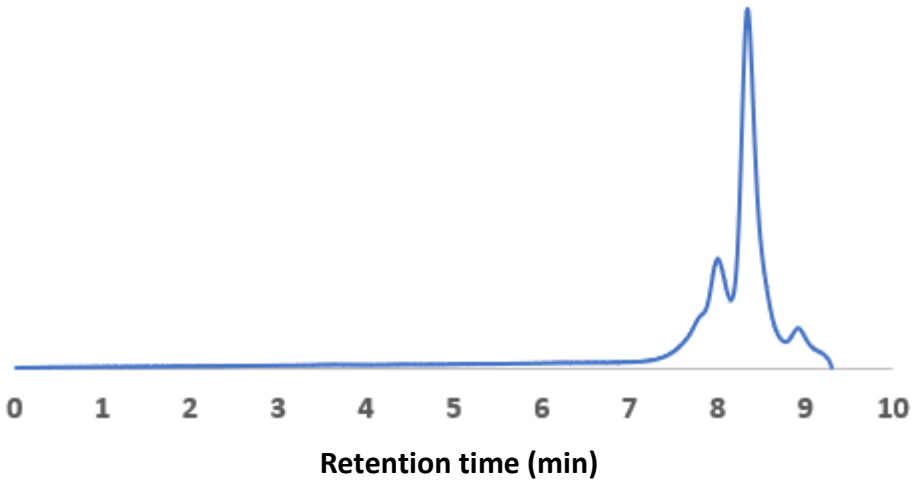

Figure S24. GPC trace of poly(EOO-*co*-SA).

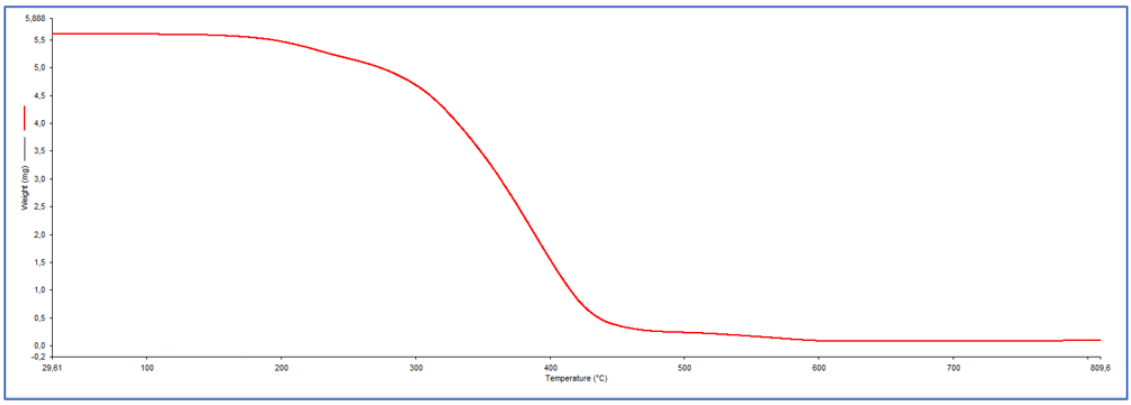

Figure S25. TGA analysis of poly(EOO-*co*-SA).

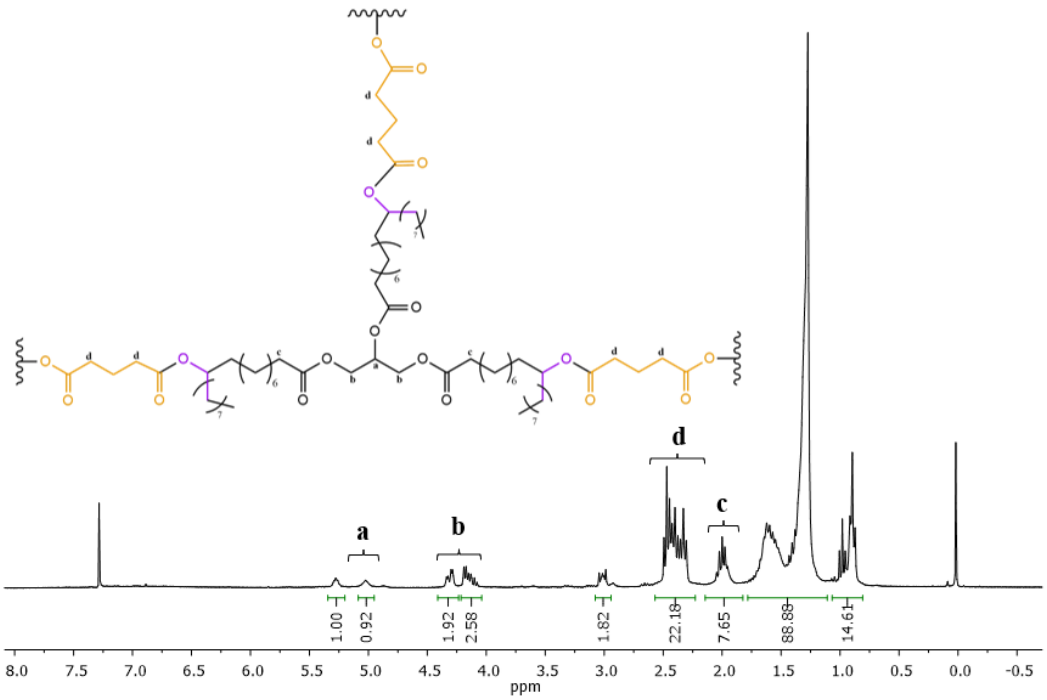

Figure S26. ^{1}H-NMR spectrum of poly(EOO-*co*-GA) in $CDCl_3$.

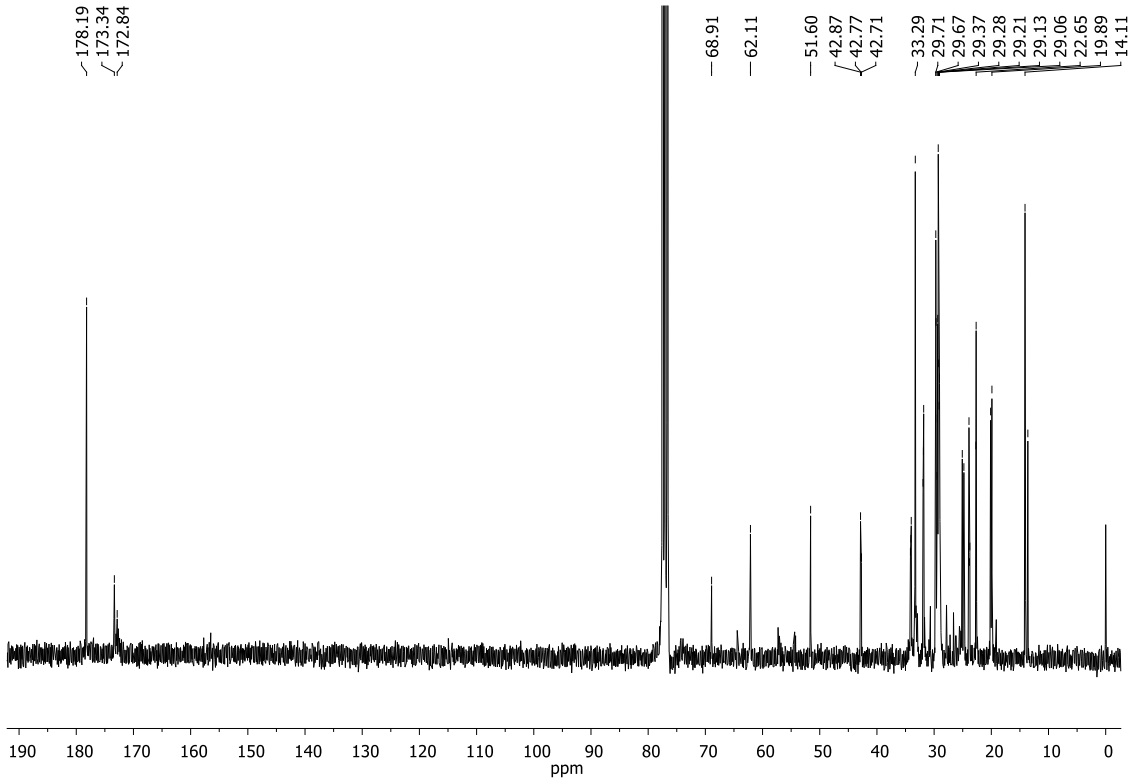

Figure S27. ^{13}C{^{1}H}-NMR spectrum of poly(EOO-*co*-GA) in $CDCl_3$.

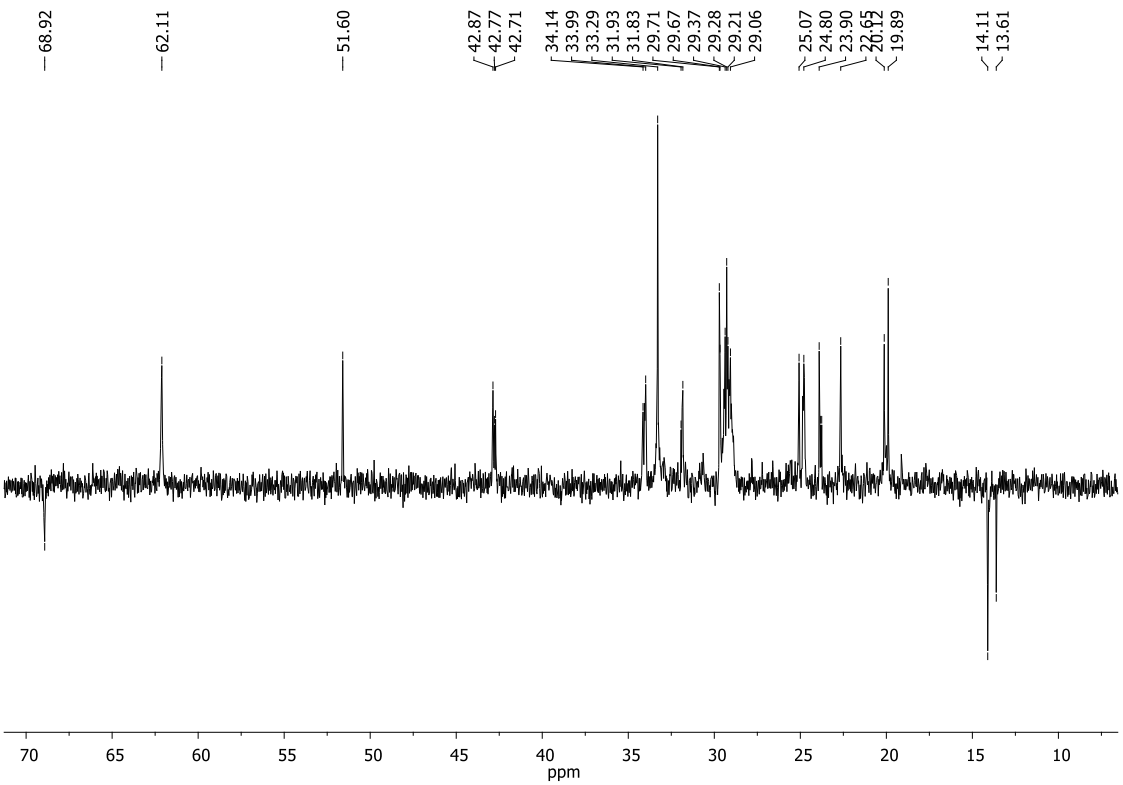

Figure S28. DEPT-NMR spectrum of poly(EOO-*co*-GA) in $CDCl_3$.

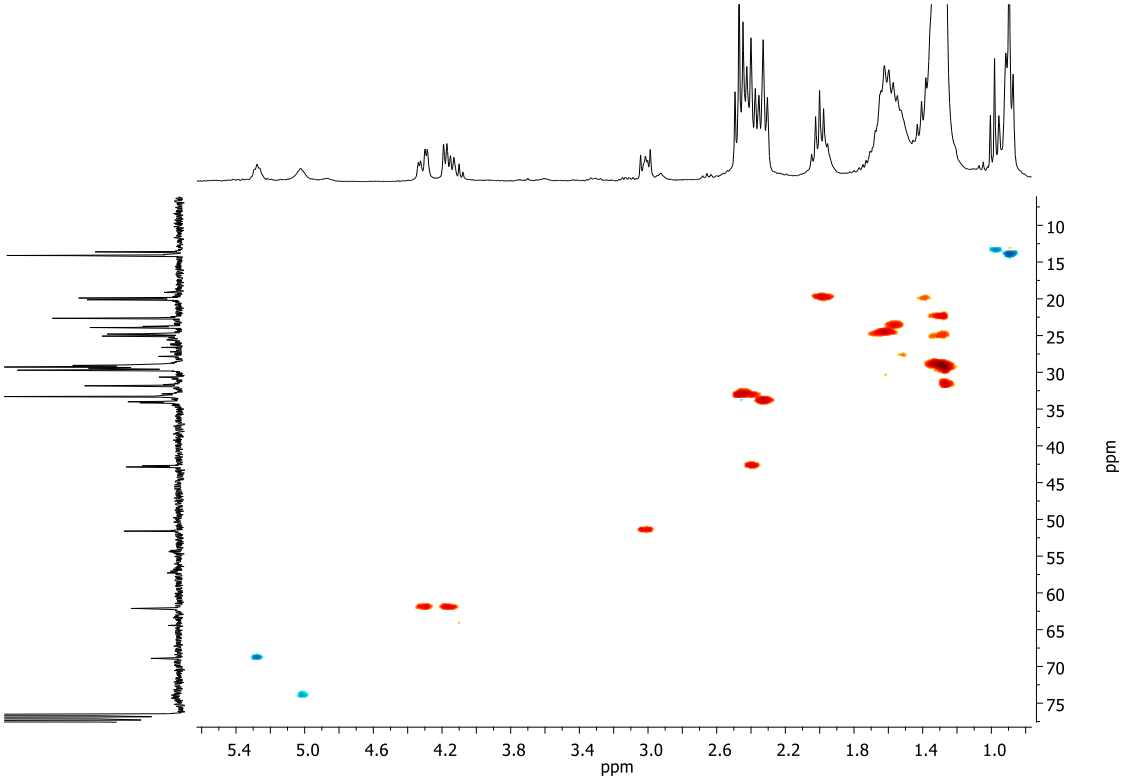

Figure S29. g-HSQC-NMR spectrum of poly(EOO-*co*-GA) in $CDCl_3$.

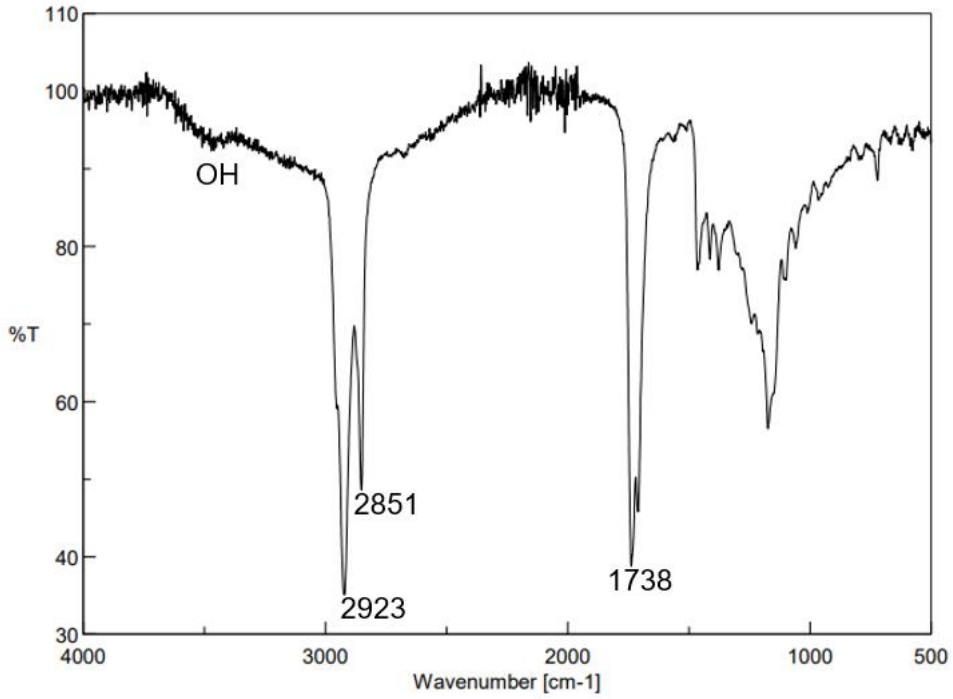

Figure S30. FT-IR spectrum of poly(EOO-*co*-GA) in $CDCl_3$.

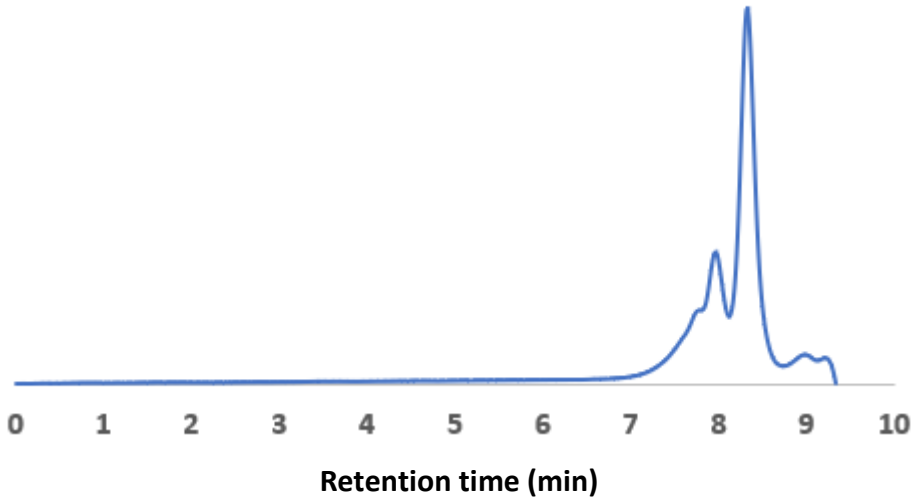

Figure S31. GPC trace of poly(EOO-*co*-GA).

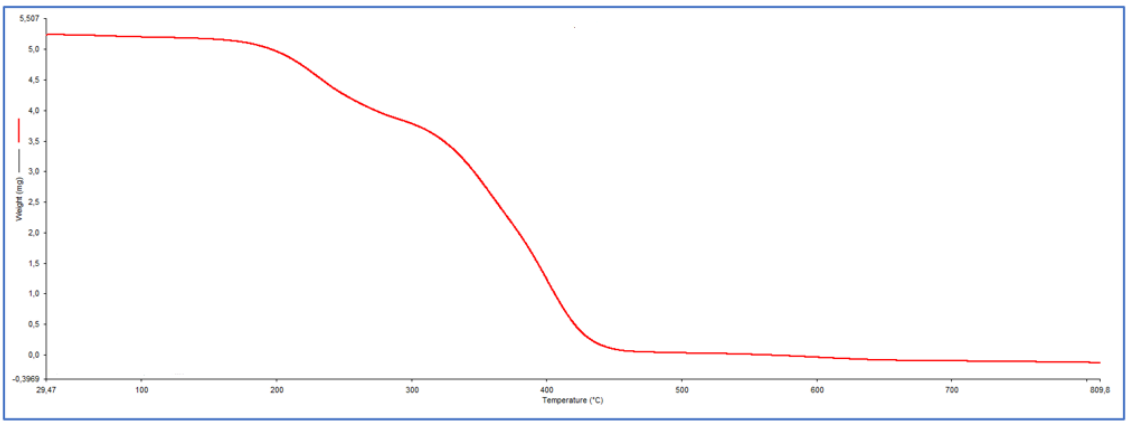

Figure S32. TGA analysis of poly(EOO-*co*-GA).

Density functional theory (DFT) calculations

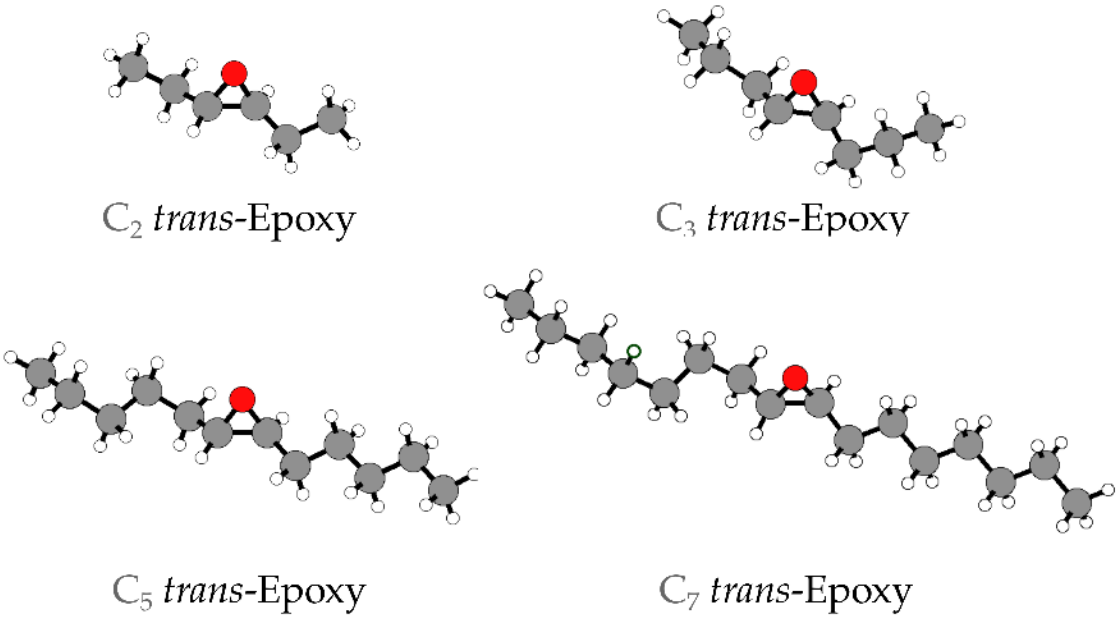

Figure S33. Final optimized geometries for a set of epoxide models containing different amounts of carbon units as side-chain. The optimization was carried out at B3LYP def2-TZVP level including the effect of the solvent (toluene) through the implicit solvent model.

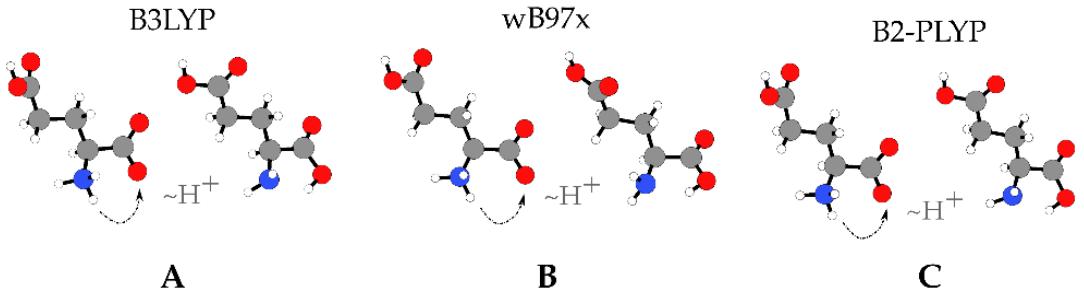

Figure S34. Initial and final structures of L-Glu molecule optimized with different DFT xc-functionals. All these optimizations predict a H transfer event from the ammonium to the carboxylate group. These simulations were performed considering toluene as solvent and including dispersion correction through D4 Grimme model.

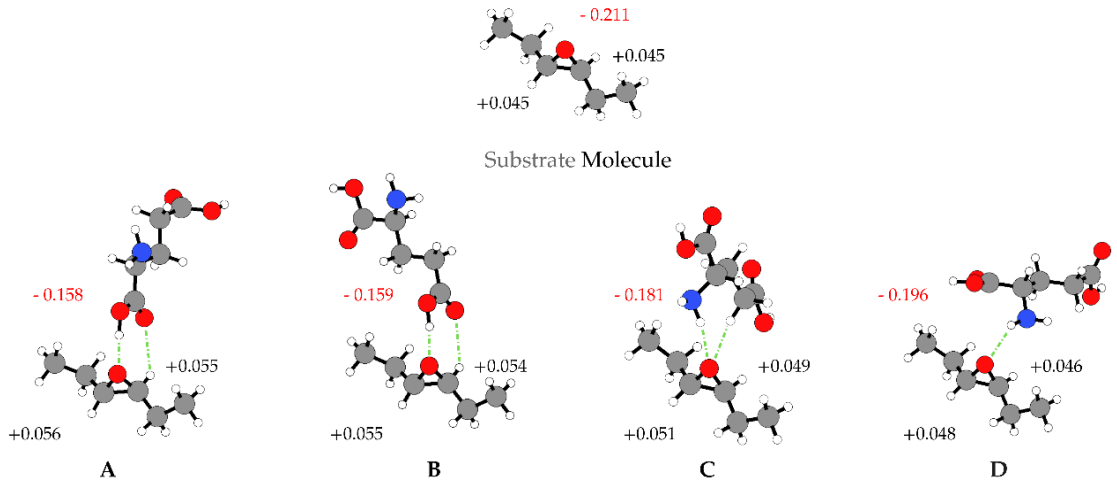

Figure S35. Optimized geometries for a set of molecular complexes identified when a single epoxide interacts with different linking point available on L-Glu molecule in vacuum.

Table S2. *Trans-cis* relative energies obtained for a set of epoxides with different side-chain sizes computed at DFT and SCS-MP2 level of theory. The obtained energies are reported in kcal mol^{-1}.

Side-chain size	B3LYP def2-TZVP	SCS-MP2 cc-pVTZ
2	**– 1.49**	**– 1.42**
3	– 1.58	– 1.47
5	– 0.64	– 0.77
7	– 0.68	– 0.89

Table S3. Hirshfeld atomic charge analysis for a set of epoxide model with different side-chain size computed at B3LYP def2-TZVP level in vacuum.

Side-chain size	Oxygen atom	Carbon 1 atom	Carbon 2 atom
2	**– 0.211**	**+ 0.045**	**+ 0.045**
3	– 0.211	+ 0.044	+ 0.045
5	–0.211	+ 0.044	+ 0.045
7	– 0.211	+ 0.044	+ 0.045

Table S4. Relative energies obtained for a set of molecular complexes identified at DFT level and recalculated at SCS-MP2 level in vacuum. The obtained energies are reported in kcal mol^{-1}.

Relative energy respect to Structure A	B3LYP def2-TZVP	SCS-MP2 cc-pVTZ
D vs A	7.38	6.15
C vs A	4.78	3.77
B vs A	0.55	0.41
A vs A	0.00	0.00